

Trajectory Modeling via Random Utility Inverse Reinforcement Learning

Anselmo R. Pitombeira-Neto
 Helano P. Santos
 anselmo.pitombeira@ufc.br
 hp@alu.ufc.br
 Insight Data Science Lab
 Federal University of Ceará
 Fortaleza, Brazil

Ticiano L. Coelho da Silva
 José Antonio F. de Macedo
 ticianalc@insightlab.ufc.br
 jose.macedo@insightlab.ufc.br
 Insight Data Science Lab
 Federal University of Ceará
 Fortaleza, Brazil

ABSTRACT

We consider the problem of modeling trajectories of drivers in a road network from the perspective of inverse reinforcement learning. As rational agents, drivers are trying to maximize some reward function unknown to an external observer as they make up their trajectories. We apply the concept of random utility from microeconomic theory to model the unknown reward function as a function of observable features plus an error term which represents features known only to the driver. We develop a parameterized generative model for the trajectories based on a random utility Markov decision process formulation of drivers decisions. We show that maximum entropy inverse reinforcement learning is a particular case of our proposed formulation when we assume a Gumbel density function for the unobserved reward error terms. We illustrate Bayesian inference on model parameters through a case study with real trajectory data from a large city obtained from sensors placed on sparsely distributed points on the street network.

KEYWORDS

Trajectory modeling, inverse reinforcement learning, random utility theory, external sensor data

1 INTRODUCTION

The ubiquity of GPS-enabled smartphones, automotive navigation systems connected to the Internet and traffic surveillance cameras have allowed the filtering and collection of large streams of trajectories from moving objects in real time. The acquired data can be used in different machine learning tasks, such as real-time detection of regularities (e.g., typical traffic flows over a road network, next location prediction in road networks) and anomalies (e.g., traffic jams), in this way aiding public or private agents in rapidly acting when confronting critical decision-making assignments in urban settings.

In this paper, we consider the problem of modeling trajectories of vehicles in a road network which are observed by external sensors located on sparse fixed points on the roadside. In contrast to the majority of previous work on trajectory modeling, in which trajectories are made up of GPS traces, trajectories from external sensors are more sparse and noisy, which makes the problem of modeling trajectories more challenging [3, 4]. While GPS traces have a high sample rate, which allows us to model trajectories as varying almost continuously over the space, external sensors are



Figure 1: Set of 272 external sensors located on the street network in the city of Fortaleza, Brazil.

placed in fixed locations and observations from the same vehicle may be very far apart.

Figure 1 illustrates the distribution of 272 external sensors in the road network of the city of Fortaleza, Brazil. These sensors scan vehicles plates mainly with the purpose of law enforcement. A vehicle trajectory is made up of a sequence of time-ordered stamps corresponding to the sequence of sensors which detected the vehicle’s plate. Figure 2 exhibits a vehicle trajectory sample. As can be seen, the distance of two consecutive sensors which detected the vehicle may range from a few meters to some kilometers, showing the sparseness of the observations.

In order to model the trajectories, we leverage concepts from inverse reinforcement learning (IRL) and random utility theory. We assume that each trajectory is generated by a driver (an agent), who interacts with the road network (the environment) and makes decisions along the way so as to maximize her total reward while trying to reach a destination. At each current location in her trajectory, the driver makes the decision of the next location to go. However, as observers of the trajectories, we do not know exactly the reward function the driver is trying to maximize.

We then apply the concept of random utility from microeconomic theory to model the unknown reward function as a function of

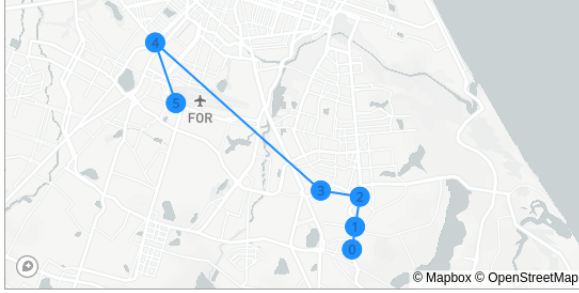


Figure 2: A sample trajectory. The distance of two consecutive sensors which detected the vehicle may range from a few meters to some kilometers.

observable features plus an error term which represents features known only to the driver. We name this approach random utility inverse reinforcement learning (RU-IRL). Thereafter, we develop a probabilistic generative model for trajectories based on RU-IRL and propose a Bayesian method to infer its parameters from a sample of observed trajectories. En passant, we also show that maximum entropy IRL, a popular IRL paradigm, is a particular case of RU-IRL when we assume a Gumbel density function for the unobserved reward error terms.

This paper is divided in the following sections: in Section 2, we review concepts on inverse reinforcement learning and random utility theory; in Section 3, we model trajectory generation by drivers as a Markov decision process (MDP); in Section 4, we detail a trajectory generative model based on the developed MDP formulation; in Section 5, we illustrate the application of the model to real trajectory data from the city of Fortaleza, Brazil; in Section 6, we list some related work; finally, we end the paper with some concluding remarks in Section 7.

2 BACKGROUND

In this section, we review the main theoretical concepts on which we base our modeling approach.

2.1 Inverse Reinforcement Learning

In (direct) reinforcement learning (RL), an agent interacts with an environment, which may be in different states at each decision epoch, and takes decisions (actions) which influences the next state of the environment. As a result of the action, the agent receives a reward. RL problems are formally described as Markov decision processes [11]. At each decision epoch t , the environment may be in one of different states $s \in \mathcal{S}$. The agent may choose an action $a \in \mathcal{A}$, after which the environment makes a transition to a new state s' according to a probability function $p(s'|s, a)$ and the agent receives a reward $r(s, a)$. A key objective in RL is to train the agent so that it maximizes the cumulative sum of rewards over a finite or infinite horizon. The behavior of the agent is synthesized in a function $\pi : \mathcal{S} \rightarrow \mathcal{A}$, called *policy*, which associates each state of the environment with an action of the agent.

In RL, the analyst designs a reward function $r(s, a)$ so as to train the agent to achieve some goal or complete a task. In contrast, in inverse reinforcement learning (IRL) the analyst observes an agent interacting with an environment and does not know exactly the reward function the agent is trying to maximize [1, 10]. The objective is to learn the behavior of the agent, i.e., its policy, through partial observations of its actions and environment states.

In our application, the agents an analyst observes are drivers and the environment is a road network. A driver executes a task of traveling between an origin and a destination and wants to achieve this efficiently in order to minimize total distance, time, or some other criteria which are unknown to the analyst. We only have access to a sequence of locations which constitute a driver's trajectory between origin and destination, detected by external sensors on the road network. Our objective is then to learn from trajectory data the parameters of an IRL-based generative model. We also use concepts from random utility theory, as introduced in the next section, to model the unknown reward function.

2.2 Random Utility Theory

Random utility theory and related *discrete choice theory* is a branch of econometrics which develops probabilistic models to explain the behavior of agents when making economic decisions [8]. In random utility theory, an agent faces a set of alternatives $a \in \mathcal{A}$, often assumed a countable set, and chooses an alternative with highest *utility* (or reward). The exact utility function is known only by the agent, so that an analyst can only observe the choices of the agent, but does not know the utility function exactly. The analyst then model the utility function as

$$R(a) = r(a) + \epsilon_a, \quad a \in \mathcal{A}, \quad (1)$$

in which $r(a)$ is the *deterministic* utility, given by

$$r(a) = \sum_{k=1}^K \phi_k(a) \beta_k,$$

$\phi_k(a)$ are features associated with each alternative and observed by the analyst, β_k are corresponding parameters and ϵ_a are error terms which account for features not observed by the analyst but known by the agent.

As the utility function (1) is a random variable, it is not possible to predict exactly the choice of the agent, but we can compute a conditional probability distribution over the alternatives which is a function of the features and depends on the probability distribution of the error terms. The conditional probability that an alternative $a \in \mathcal{A}$ is chosen by the agent is given by

$$p(a|\theta) = \Pr\{R(a) \geq R(a')\}, \quad \forall a, a' \in \mathcal{A},$$

and θ is a vector which collects all parameters including $\beta_k, k \in \{1, 2, \dots, K\}$.

When error terms are assumed to be independent and identically distributed with a Gumbel density function (extreme value type I), one obtains the celebrated *multinomial logit* model, with probability function over alternatives given by

$$p(a|\theta) = \frac{e^{r(a)/\alpha}}{\sum_{a' \in \mathcal{A}} e^{r(a')/\alpha}}, \quad \forall a \in \mathcal{A}, \quad (2)$$

in which $\alpha > 0$ is the scale parameter of the Gumbel error terms with expected values equal to zero. It can also be shown that the expected value of the maximum utility is given by the *logsumexp* formula

$$\mathbb{E} \left[\max_{a \in \mathcal{A}} R(a) \right] = \alpha \ln \left(\sum_{a \in \mathcal{A}} e^{r(a)/\alpha} \right). \quad (3)$$

We can build alternative probability models, such as the multinomial probit, nested logit and mixed logit, depending on the probability distributions assumed for the error terms, although we stick with the multinomial logit in this paper. We refer to [8] for further theory on random utility models.

3 MARKOV DECISION PROCESS FORMULATION

Hereafter, we model trajectory generation by drivers as a Markov decision process. We consider a set \mathcal{S} of locations (the states of the environment) through which a vehicle may travel during its trajectory from an origin to a destination. We assume each location has an external sensor by which a vehicle is detected if its trajectory includes the location. The observed trajectory of a vehicle consists of a sequence of locations identified by the corresponding sensors $\langle s_0, s_2, \dots, s_n \rangle$, in which $o = s_0$ is the observed origin of the vehicle and $d = s_n$ is its observed destination.

We assume that, when a vehicle is detected at a sensor $s_t \in \mathcal{S}$ at a time t (i.e., it is in the geographical region the sensor is located), the driver chooses a next location $a_t \in \mathcal{A}_s$ as part of its trajectory to reach the destination, in which \mathcal{A}_s denotes the reachable locations from s . In its next location, the vehicle will likely be detected by a sensor s_{t+1} , with probability $p(s_{t+1}|s_t, a_t)$. Notice that the destination d is assumed to be an *absorbing* state, so that $p(s_{t+1}|s_t = d, a_t) = 0, \forall s_{t+1} \neq d, \forall a \in \mathcal{A}_s$.

In the particular application we are interested, we observe the locations of the vehicles by means of sensors in fixed positions on the roadside. These sensors can track the trajectories of particular vehicles through plate scanning. As we only observe the states but do not observe the drivers decisions, we make the following assumptions: At a state s , the driver makes a decision $a \in \mathcal{A}_s$ in which \mathcal{A}_s is the set of achievable locations from current location s ; and if the driver chooses to go to a location s' , then it almost surely will be detected by the sensor located in s' , i.e., $p(s'|s, a) = 1$ if $s' = a$, and $p(s'|s, a) = 0$ if $s' \neq a$. In other words, the next state s' is a deterministic function of the decision.

However, in order to properly take into account the unobserved features represented in the error terms ϵ as in the random utility function (1), we consider an *extended state* (s, ϵ) , which is fully visible to the driver, but the analyst can see only the locations s detected by the sensors. The part of the state corresponding to ϵ represents information that only the agent has access. Under the extended state, the reward function is given by

$$R(s, \epsilon, s') = r(s, s') + \epsilon, \quad (4)$$

in which $r(s, s')$ is the deterministic part of the reward related to the action of going to location s' , given by

$$r(s, s') = \sum_{k=1}^K \phi_k(s, s') \beta_k. \quad (5)$$

Algorithm 1 Fixed-point iteration to compute v_θ

Input: Set $\mathcal{S}, \mathcal{A}_s \forall s \in \mathcal{S}$, reward function $r(s, s')$, destination d , parameters $\theta = (\alpha, \beta, \gamma)$

- 1: **initial step** Set $v_\theta^{(0)}(s) \leftarrow 0, \forall s \in \mathcal{S}, j \leftarrow 0$
- 2: **while** True **do**
- 3: **for** $s \in \mathcal{S}, s \neq d$ **do**
- 4: $v_\theta^{(j+1)}(s) \leftarrow \alpha \ln \left(\sum_{s' \in \mathcal{A}_s} e^{[r(s, s') + \gamma v_\theta^{(j)}(s')]/\alpha} \right)$
- 5: **end for**
- 6: **if** $\|v_\theta^{(j+1)} - v_\theta^{(j)}\|_\infty < \xi$ **then**
- 7: $v_\theta^\xi \leftarrow v_\theta^{(j+1)}$
- 8: **break**
- 9: **else**
- 10: $j \leftarrow j + 1$
- 11: **end if**
- 12: **end while**
- 13: **return** v_θ^ξ ▷ ξ -approximate value function

An optimal policy followed by an agent is greedy in relation to an optimal value function v^* , which satisfies Bellman's equation

$$v^*(s, \epsilon) = \max_{s' \in \mathcal{A}_s} \left\{ r(s, s') + \epsilon + \gamma \mathbb{E}_{\epsilon' \sim p(\epsilon')} [v^*(s', \epsilon')] \right\}, \quad (6)$$

in which $p(\epsilon')$ is the probability distribution of the errors (assumed i.i.d) and $0 < \gamma \leq 1$ is a discount factor. In addition, notice that the optimal value function (6) is a random variable. We then further work with its expected value

$$v_\theta(s) = \mathbb{E}_{\epsilon \sim p(\epsilon)} [v^*(s, \epsilon)]$$

and from (6) we have

$$v_\theta(s) = \mathbb{E}_{\epsilon \sim p(\epsilon)} \left[\max_{s' \in \mathcal{A}_s} \left\{ r(s, s') + \epsilon + \gamma v_\theta(s') \right\} \right], \forall s \in \mathcal{S}$$

in which θ is a vector of parameters and we have omitted the dependence of $r(s, s')$ on θ . If we assume that the errors ϵ are i.i.d Gumbel variables with zero mean and scale factor α , then from Eq. (3)

$$v_\theta(s) = \alpha \ln \left(\sum_{s' \in \mathcal{A}_s} e^{[r(s, s') + \gamma v_\theta(s')]/\alpha} \right), \quad \forall s \in \mathcal{S}. \quad (7)$$

This is, the expected value function v_θ is the fixed point of the operator defined by the right-hand side of (7). It can be shown that this operator is a contraction, so that the value function v_θ , according to Banach's fixed point theorem, may be found by fixed point iteration [13]. In our application, as we treat the destination d as an absorbing state, we define $v_\theta(d) = 0$, so that v_θ is also a function of d . (In further developments below we assume conditioning on d is implicit.) Algorithm 1 describes a fixed-point iteration (akin to value-iteration) to compute the value function v_θ .

Finally, under the aforementioned assumptions and according to Eq. (2), we can show that the conditional probability that a driver goes to location s' , given that it is currently at location s during a trajectory $\langle s_0, s_1, \dots \rangle$ with origin $o = s_0$ and destination d is

$$p(s'|s, o, d, \theta) = \frac{e^{[r(s, s') + \gamma v_\theta(s')]/\alpha}}{\sum_{s'' \in \mathcal{A}_s} e^{[r(s, s'') + \gamma v_\theta(s'')]/\alpha}}, \forall s' \in \mathcal{S}. \quad (8)$$

Notice that the choice probability given by (8) has the same mathematical form as a stochastic policy known as Boltzmann exploration in RL literature. However, in our modeling the interpretation is different: the agent is not following a stochastic policy, but rather it is following an optimal deterministic policy (a greedy policy in relation to the optimal value function given by Bellman’s equation (6)) which *appears* to us as stochastic because we do not fully observe the extended state (s, ϵ) .

4 TRAJECTORY GENERATIVE MODEL

From the Markov decision process formulation of the trajectory generation process, we can directly conceive a probabilistic generative model for trajectories, according to the following steps:

- (1) Generate an origin-destination pair $(o, d) \sim p(o, d)$;
- (2) Compute value function $v_\theta(s)$, $\forall s \in \mathcal{S}$, with $v_\theta(d) = 0$;
- (3) Generate a trajectory $\tau = \langle s_0, s_1, s_2, \dots, s_n \rangle$, with $o = s_0$ and $d = s_n$, by sampling each next sensor s_{t+1} from conditional probability (8) until destination d (which is an absorbing state) is reached;

in which $p(o, d)$ is the probability of a trip between origin-destination pair (o, d) and value function $v_\theta(s)$, $\forall s \in \mathcal{S}$ is computed by using Algorithm 1 with given parameters θ . Notice that this generative model can generate trajectories with cycles and there is no upper bound on the length of a trajectory, although we could put an upper bound by simply reject sampling generated trajectories larger than some desired bound.

From a parameter inference perspective, it will be useful to obtain the conditional probability of a trajectory τ , given an (o, d) pair and the parameters θ :

$$\begin{aligned} p(\tau|o, d, \theta) &= \prod_{t=0}^{n-1} p(s_{t+1}|s_t, o, d, \theta) \\ &= \prod_{t=0}^{n-1} \frac{e^{[r(s_t, s_{t+1}) + \gamma v_\theta(s_{t+1})]/\alpha}}{\sum_{s' \in \mathcal{A}_{s_t}} e^{[r(s_t, s') + \gamma v_\theta(s')]/\alpha}}. \end{aligned} \quad (9)$$

In the case $\gamma = 1$, we can show that (9) simplifies according to the following proposition:

PROPOSITION 4.1. *If $\gamma = 1$, the probability of a trajectory $\tau = \langle s_0, s_1, s_2, \dots, s_n \rangle$ is given by*

$$p(\tau|o, d, \theta) = \frac{e^{\sum_{t=0}^{n-1} r(s_t, s_{t+1})/\alpha}}{e^{v_\theta(s_0)/\alpha}}. \quad (10)$$

The proof of Proposition 4.1 may be found in Appendix A. Notice that (10) corresponds to the maximum entropy probability distribution over trajectories as proposed in [20], in which $e^{v_\theta(s_0)/\alpha}$ is the normalization constant over the countable set of possible trajectories between (o, d) pair. In this way, maximum entropy IRL is a particular case of random utility IRL corresponding to the assumption of a Gumbel density function for the unobserved errors in the reward function (4) and discount factor $\gamma = 1$.

4.1 Parameter Estimation

Given a set of observed trajectories $\mathcal{T} = \{\tau_i\}_{i=1}^m$, assuming the trajectories are independent, the likelihood function of the data is

given by

$$p(\mathcal{T}|\theta) = \prod_{i=1}^m p(\tau_i|o_i, d_i, \theta),$$

in which $p(\tau_i|o_i, d_i, \theta)$ is given by (9).¹ The parameters θ may be estimated by standard techniques such as maximum likelihood or Bayesian inference.

A natural question arises regarding identifiability of parameters in this model, on which we present the following important result:

PROPOSITION 4.2. *Scaling both parameters α and β by a constant $b \neq 0$ does not change the likelihood of a trajectory τ .*

The proof of Proposition 4.2 may be found in Appendix A. Proposition ?? implies that we cannot estimate the exact values of both parameters β and α , even if we have an infinite sample. Only the ratios $\beta_1/\alpha, \beta_2/\alpha, \dots$ are identifiable, so that we can freely set the values of parameter α and focus only on estimating β . Although in principle we could also try to estimate γ , since we are working in an episodic setting (a trajectory ends when the agent reaches the destination), we assume $\gamma = 1$ henceforth.

Let us consider Bayesian inference on β , assuming $\alpha = \gamma = 1$. Given a set of observed trajectories $\mathcal{T} = \{\tau_i\}_{i=1}^m$, the posterior probability distribution is given by

$$p(\beta|\mathcal{T}) \propto \prod_{i=1}^m p(\tau_i|o_i, d_i, \beta)p(\beta),$$

in which $p(\tau_i|o_i, d_i, \beta)$ is given by (10). Since there is no conjugate posterior distribution, we must resort to simulation or variational techniques. We consider using a posterior sampler based on the Metropolis-Hastings method [6], given in Algorithm 2. Moreover, notice that, at each iteration of the Metropolis-Hastings algorithm, we have to compute the value function by applying Algorithm 1.

4.2 Online Next Location Prediction

A frequent task in trajectory modeling is *online next location prediction*, in which we want to estimate the next location of an agent at time $t + 1$ having observed previous locations up to time t . Given a partial trajectory $\langle o = s_0, s_1, \dots, s_t \rangle$, we want to compute the marginal predictive probability

$$p(s'|s_{0:t}, \mathcal{T}), \quad s' \in \mathcal{A}_{s_t}, \quad (11)$$

in which s' are the possible next locations and \mathcal{T} is a set of previously observed full trajectories. Thereafter, we can predict the next location as

$$\hat{s} = \arg \max_{s' \in \mathcal{A}_{s_t}} p(s'|s_{0:t}, \mathcal{T}). \quad (12)$$

¹We notice that, more rigorously, we should condition on the (o, d) pairs and write $p(\mathcal{T}|(o_1, d_1), (o_2, d_2), \dots, (o_m, d_m), \theta)$, but since the (o, d) pairs are assumed to be observed in the trajectories, we have that the marginal $p(\mathcal{T}|\theta) = p(\mathcal{T}|(o_1, d_1), (o_2, d_2), \dots, (o_m, d_m), \theta)$.

Algorithm 2 Metropolis-Hastings for sampling from $p(\boldsymbol{\beta}|\mathcal{T})$

Input: Set \mathcal{S} , $\mathcal{A}_s \forall s \in \mathcal{S}$, reward function $r(s, s')$, set of trajectories \mathcal{T} , set of destinations \mathcal{D} , prior distribution $p(\boldsymbol{\beta})$, proposal distribution $g(\boldsymbol{\beta}'|\boldsymbol{\beta})$

- 1: **initial step** Set initial $\boldsymbol{\beta}^{(0)}$, $v^d(s)^{(0)} \leftarrow v_{\boldsymbol{\beta}^{(0)}}^d(s), \forall s \in \mathcal{S}, d \in \mathcal{D}$, $j \leftarrow 0$
- 2: **repeat**
- 3: Sample candidate $\boldsymbol{\beta}' \sim g(\boldsymbol{\beta}|\boldsymbol{\beta}^{(j)})$
- 4: Compute $v_{\boldsymbol{\beta}'}^d(s), \forall s \in \mathcal{S}, d \in \mathcal{D}$ ▷ Alg. 1
- 5: Compute acceptance ratio

$$\rho = \min \left\{ \frac{\prod_{i=1}^m p(\tau_i|o_i, d_i, \boldsymbol{\beta}') p(\boldsymbol{\beta}') g(\boldsymbol{\beta}^{(j)}|\boldsymbol{\beta}')}{\prod_{i=1}^m p(\tau_i|o_i, d_i, \boldsymbol{\beta}^{(j)}) p(\boldsymbol{\beta}^{(j)}) g(\boldsymbol{\beta}'|\boldsymbol{\beta}^{(j)})}, 1 \right\}$$
- 6: Sample $u \sim \text{unif}(0, 1)$
- 7: **if** $u < \rho$ **then**
- 8: $\boldsymbol{\beta}^{(j+1)} \leftarrow \boldsymbol{\beta}'$,
- 9: $v^d(s)^{(j+1)} \leftarrow v_{\boldsymbol{\beta}'}^d(s), \forall s \in \mathcal{S}, d \in \mathcal{D}$
- 10: **else**
- 11: $\boldsymbol{\beta}^{(j+1)} \leftarrow \boldsymbol{\beta}^{(j)}$,
- 12: $v^d(s)^{(j+1)} \leftarrow v^d(s)^{(j)}, \forall s \in \mathcal{S}, d \in \mathcal{D}$
- 13: **end if**
- 14: $j \leftarrow j + 1$
- 15: **until** Convergence
- 16: **return** Posterior sample $\boldsymbol{\beta}^{(0)}, \boldsymbol{\beta}^{(1)}, \dots$

Notice that the predictive probability (11) can be obtained by marginalizing over the parameters $\boldsymbol{\beta}$ and destinations d :

$$\begin{aligned} p(s'|s_{0:t}, \mathcal{T}) &= \frac{p(s', s_{1:t}|s_0, \mathcal{T})}{p(s_{1:t}|s_0, \mathcal{T})} \\ &= \frac{\int \sum_{d \in \mathcal{D}} p(s', s_{1:t}, d, \boldsymbol{\beta}|s_0, \mathcal{T}) d\boldsymbol{\beta}}{\int \sum_{d \in \mathcal{D}} p(s_{1:t}, d, \boldsymbol{\beta}|s_0, \mathcal{T}) d\boldsymbol{\beta}} \\ &= \frac{\int \sum_{d \in \mathcal{D}} p(s'|s_t, d, \boldsymbol{\beta}) p(s_{1:t}|s_0, d, \boldsymbol{\beta}) p(d|s_0, \mathcal{T}) p(\boldsymbol{\beta}|\mathcal{T}) d\boldsymbol{\beta}}{\int \sum_{d \in \mathcal{D}} p(s_{1:t}|s_0, d, \boldsymbol{\beta}) p(d|s_0, \mathcal{T}) p(\boldsymbol{\beta}|\mathcal{T}) d\boldsymbol{\beta}}, \end{aligned} \quad (13)$$

in which

$$p(s_{1:t}|s_0, d, \boldsymbol{\beta}) = \prod_{i=0}^{t-1} p(s_{i+1}|s_i, d, \boldsymbol{\beta}),$$

\mathcal{D} is a set of possible destinations, $p(s_{i+1}|s_i, d, \boldsymbol{\beta})$ is given by Eq. (8), $p(d|s_0, \mathcal{T})$ is the conditional distribution of the destination of the current partial trajectory given its observed origin and $p(\boldsymbol{\beta}|\mathcal{T})$ is the posterior distribution of $\boldsymbol{\beta}$ given the training data.

Moreover, notice that the integral in (13) will hardly be solvable, so we resort to a Monte Carlo estimator. Given a sample $(\boldsymbol{\beta}^{(1)}, \boldsymbol{\beta}^{(2)}, \dots, \boldsymbol{\beta}^{(n)})$ drawn from the posterior $p(\boldsymbol{\beta}|\mathcal{T})$, we may approximate (13) by substituting the integrals for sums over the sample:

$$\hat{p}(s'|s_{0:t}, \mathcal{T}) = \frac{\sum_{i=1}^n \sum_{d \in \mathcal{D}} p(s'|s_t, d, \boldsymbol{\beta}^{(i)}) p(s_{1:t}|s_0, d, \boldsymbol{\beta}^{(i)}) p(d|s_0, \mathcal{T})}{\sum_{i=1}^n \sum_{d \in \mathcal{D}} p(s_{1:t}|s_0, d, \boldsymbol{\beta}^{(i)}) p(d|s_0, \mathcal{T})}. \quad (14)$$

We can obtain a sample from $p(\boldsymbol{\beta}|\mathcal{T})$ by means of Algorithm 2.

5 CASE STUDY

We applied our model to real data obtained from 272 external sensors in the urban road network from the city of Fortaleza, Brazil, which is the fifth largest city in Brazil with a population of about 3 million people (See Figure 1). The data correspond to car plates scanned during a time window between 4:00 p.m. and 8:00 p.m. on a Friday in September 2017. For each anonymized car plate, the data consists of the sequence of sensors which detected the plate and their corresponding timestamps.

Besides data cleaning, the main preprocessing operation we have carried out was to identify trips within a trajectory stream. We have used the cutoff of 30 min to split a trajectory stream into separate trips, i.e., when two consecutive timestamps have a time difference greater than 30 min, we considered that this indicates that these correspond to two (or more) different trips. The specific cutoff value was chosen since, given prior knowledge on trip times in the road network of the city of Fortaleza, it is unlikely that a vehicle spends more than 30 min without being detected by any sensor. We also discarded short trips with less than 6 observations, amounting to a total of 48920 trip trajectories. Finally, we have divided the dataset in a 80/20% training/test split.

We considered two features in the reward function (see Eq. (5)): the length of the shortest path in the road network between locations s and s' , and the average travel time between locations s and s' , corresponding, respectively, to parameters $\boldsymbol{\beta} = (\beta_1, \beta_2)$. We applied Algorithm 2 to the training data \mathcal{T} in order to sample from the posterior $p(\boldsymbol{\beta}|\mathcal{T})$. We used uninformative flat priors over $[0, +\infty)$ for both β_1 and β_2 and used a bivariate Gaussian proposal distribution $g(\boldsymbol{\beta}'|\boldsymbol{\beta}^{(j)}) = \mathcal{N}(\boldsymbol{\beta}^{(j)}, \Sigma)$ with a diagonal covariance matrix $\Sigma = \text{diag}(\sigma_1^2, \sigma_2^2)$. We applied an adaptive procedure to tune the variances σ_1^2 and σ_2^2 of the proposal distribution in order to maintain the acceptance rate at reasonable levels. We ran previously a vanilla Bayesian optimization algorithm to find good starting values in a high density region. We let the Markov chain run for 10^4 iterations. Figures 3 and 4 illustrate, respectively, the Markov chain and a histogram of the samples.

It is surprising that β_1 is very close to zero, indicating that the time between locations is the main feature drivers are taking into account during their trajectories (we have adjusted distance and time data to equivalent scales). This makes sense if we take into account that during peak hours, in which traffic congestion is high, shortest paths in the network are not necessarily the fastest.

We further investigated the application of our model to the next location prediction task. For each of the 9784 trajectories in the holdout sample and each location in the trajectories, we set the prediction for the next location from Eq. (12), with posterior predictive probability computed from Eq. (14) with a sample of posterior values for $\boldsymbol{\beta}$ obtained from the simulated Markov chain shown in Figure 3. Notice that in (14) we have to provide $p(d|s_0, \mathcal{T})$. We consider two cases: in the first one, denoted as the informed case, we approximate the conditional probabilities of the destinations by computing the relative frequencies of each destination given the possible origins in the training data \mathcal{T} ; in the second one, denoted as the uninformed case, we simply use a uniform distribution over the possible destinations.

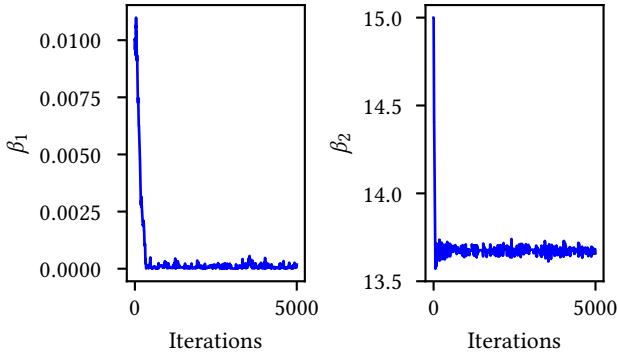


Figure 3: Markov chain generated by Algorithm 2. Starting values were 0.01 and 15.0 for β_1 and β_2 , respectively, obtained by running a Bayesian optimization algorithm for some iterations. For better visualization, only the first 5×10^3 samples are shown

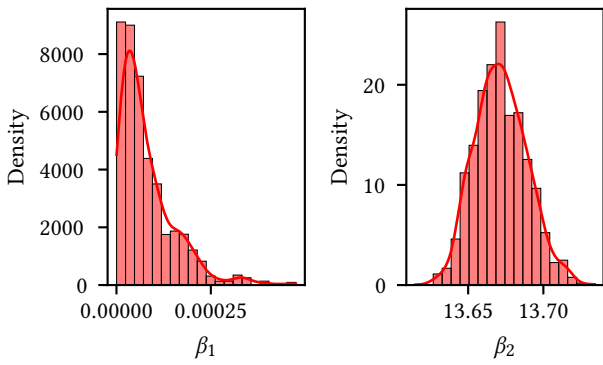


Figure 4: Histograms of 5×10^3 samples in the left tail of the Markov chain generated by Alg. 2. Posterior means for β_1 and β_2 are 7.947×10^{-5} and 13.67, respectively

We have compared our approach with alternative baselines, namely: a nearest-neighbor predictor, in which the predicted next location is simply the closest one according to road distance; a nearest-neighbor based on travel time; a first-order Markov predictor, which returns the predicted location as the most probable with probabilities estimated from the relative frequencies of transitions between locations observed in the training data \mathcal{T} ; and a random predictor, which samples uniformly among the 10 nearest neighbors (according to distance) of the current location.

We used the accuracy of the predictions as a performance metric, defined as the number of locations correctly predicted over the total number of locations observed in all trajectories in the holdout sample. We also report $\text{Acc}_{<0.5}$ ($\text{Acc}_{<1.0}$), which counts an incorrectly predicted location within 0.5 km (1.0 km) of the correct location as a success. These metrics are important from a practical standpoint,

Table 1: Accuracy of online next location prediction methods (in %) in the holdout sample of 9784 trajectories, with a total of 65612 observed locations (average of 5 train-test splits with different seeds). RU-IRL: Random utility inverse reinforcement learning; (inf.) and (uninf.) refer to the informed and uninform cases, respectively; NN: Nearest Neighbor

Method	Acc	Acc _{<0.5}	Acc _{<1.0}
RU-IRL (inf.)	69.57	74.70	77.83
RU-IRL (uninf.)	64.52	69.45	72.53
NN (distance)	20.74	29.59	39.28
NN (time)	58.70	62.73	65.21
Markov	74.10	78.81	81.51
Random	8.07	12.98	20.65

since a prediction error of up to 0.5 km may still be acceptable in a real application. Table 1 exhibits the results.

The predictions obtained via the RU-IRL method were more accurate than baseline methods, except for the Markov predictor, which was remarkably accurate. A possible explanation for this result is that the Markov predictor uses the empirical conditional probability distribution of the transitions between locations, which also captures other features in the data other than distance and time not accounted for in the RU-IRL model. On the other hand, learning Markov models requires in general large amounts of data due to the *zero frequency problem* [2], and the good performance of the Markov model may be due to the large sample of trajectories used.

It is also worth noting that the uninformative RU-IRL method achieved good performance despite being much less flexible, with only two estimated parameters (β_1 and β_2), while the number of estimated parameters of the Markov method corresponds to the number of transition probabilities (272×271 possible transitions). This is also in accordance with results obtained by [4], in which a recurrent neural network with both location and timestamp inputs achieved only a slightly better performance than a first-order Markov model in the next location prediction task.

6 RELATED WORK

Trajectory modeling and prediction has attracted a lot of attention in recent years and we cite below a selection of papers which are somewhat related to our work. In contrast to our approach, most of them apply black box models such as artificial neural networks.

In [4], the authors propose a recurrent neural network model to predict the next location from moving object trajectories captured by external sensors (e.g., traffic surveillance cameras) placed on the roadside. They also cope with the incompleteness and sparsity problems that are inherent to trajectories captured by sensors, and propose a scheme to integrate the solutions to such problems into the prediction model. In [3], the authors also tackle the next location prediction problem, however, instead of a single task model, they propose a recurrent multi-task learning approach that uses both temporal and spatial information in the training phase to jointly learn more meaningful representations of time and space.

The papers [15] and [16] use trajectory data over a road network to train a recurrent neural network to model trajectories and predict the next location. However, these works consider dense trajectories from GPS data, that, unlike the trajectory data captured by external sensors, do not present sparseness or incompleteness problems. In [12] it is proposed a suffix-tree to predict the next stop and the leave time from the actual location. The work [9] predicts the next location by grouping users who share similar characteristics and uses sequential rules to estimates the probability of visiting a specific location given the recent movement of the user and his group.

GMove [18] is an ensemble of Hidden Markov Models (HMM) to model trajectories and predict next location. GMove uses spatiotemporal information and geo-tagged text extracted from online check-ins with each HMM based on a group of users sharing similar movements. MyWay[14] predicts the next position based on the spatial match of trajectories to a set of profiles obtained by clustering raw trajectories. DeepMove [5] uses recurrent neural networks with attention layer to predict the stop of a moving object on the next time window. [7] proposed a recurrent neural network to predict the next location considering continuous spatial and temporal features. SERM [17] is a spatiotemporal model based on recurrent networks to predict the next stop that uses semantic trajectories obtained from social media. Finally, TA-TEM [19] predicts the next stop by learning from sequence of check-ins considering temporal and general user preferences.

7 CONCLUDING REMARKS

We developed an approach based on random utility inverse reinforcement learning for modeling trajectories of drivers in a road network which are observed by sensors sparsely distributed. We considered unobserved features in the reward function as making part of an extended state, which we modeled as following a Gumbel density function, and proposed a generative model for trajectories. We demonstrated that maximum entropy inverse reinforcement learning is a particular case of random utility inverse reinforcement learning. We also developed Bayesian inference on model parameters and illustrated the application of the model to real data obtained from 272 sensors in the city of Fortaleza, Brazil. The generative model can be extended by adding more levels to the hierarchical structure or using distributions other than the Gumbel density. For instance, taste variation among drivers may be incorporated by assuming that parameters related to features are random according to a probability distribution higher in the hierarchy. Other further extension is to model measurement errors in the sensors by explicitly assuming that exact locations of drivers are hidden and only partially observed through imprecise measurements.

ACKNOWLEDGMENTS

This work was partially supported by the Secretaria Nacional de Segurança Pública - Brazil (SENASP). The work of Anselmo R. Pitombeira-Neto was also supported by the Conselho Nacional de Desenvolvimento Científico e Tecnológico (CNPq) under grant number 422464/2016-3.

REFERENCES

- [1] Pieter Abbeel and Andrew Y Ng. 2004. Apprenticeship learning via inverse reinforcement learning. In *Proceedings of the Twenty-First International Conference on Machine Learning*. 1.
- [2] Ron Begleiter, Ran El-Yaniv, and Golan Yona. 2004. On prediction using variable order Markov models. *Journal of Artificial Intelligence Research* 22 (2004), 385–421.
- [3] Livia Almada Cruz, Karine Zeitouni, Ticiana Linhares Coelho da Silva, José Antonio Fernandes de Macedo, and José Soares da Silva. 2020. Location prediction: a deep spatiotemporal learning from external sensors data. *Distributed and Parallel Databases* (2020), 1–22.
- [4] Livia Almada Cruz, Karine Zeitouni, and José Antonio Fernandes de Macedo. 2019. Trajectory Prediction from a Mass of Sparse and Missing External Sensor Data. In *Proceedings of the 20th IEEE International Conference on Mobile Data Management (MDM)*. IEEE, 310–319.
- [5] Jie Feng, Yong Li, Chao Zhang, Funing Sun, Fanchao Meng, Ang Guo, and Depeng Jin. 2018. DeepMove: Predicting Human Mobility with Attentional Recurrent Networks. In *Proceedings of the 2018 World Wide Web Conference on World Wide Web*. International World Wide Web Conferences Steering Committee, 1459–1468.
- [6] W. K. Hastings. 1970. Monte Carlo sampling methods using Markov chains and their applications. *Biometrika* 57, 1 (04 1970), 97–109. <https://doi.org/10.1093/biomet/57.1.97> arXiv:<https://academic.oup.com/biomet/article-pdf/57/1/97/23940249/57-1-97.pdf>
- [7] Qiang Liu, Shu Wu, Liang Wang, and Tieniu Tan. 2016. Predicting the Next Location : A Recurrent Model with Spatial and Temporal Contexts. In *Proceedings of the 30th Conference on Artificial Intelligence (AAAI 2016)*, 194–200. <https://doi.org/10.1016/j.egypro.2016.11.209> arXiv:[arXiv:1011.1669v3](https://arxiv.org/abs/1011.1669v3)
- [8] Daniel McFadden. 1981. Econometric models of probabilistic choice. *Structural analysis of discrete data with econometric applications* 198272 (1981).
- [9] Elahe Naserian, Xinheng Wang, Keshav Dahal, Zhi Wang, and Zaijian Wang. 2018. Personalized location prediction for group travellers from spatial-temporal trajectories. *Future Generation Computer Systems* 83 (2018), 278–292. <https://doi.org/10.1016/j.future.2018.01.024>
- [10] Andrew Y. Ng and Stuart J. Russell. 2000. Algorithms for Inverse Reinforcement Learning. In *Proceedings of the Seventeenth International Conference on Machine Learning (ICML '00)*. Morgan Kaufmann Publishers Inc., San Francisco, CA, USA, 663–670.
- [11] Martin L. Puterman. 1994. *Markov Decision Processes: Discrete Stochastic Dynamic Programming*. John Wiley & Sons, Inc., USA.
- [12] Cleilton L. Rocha, Igo R. Brilhante, Francesco Lettich, Jose Antônio F. De Macedo, Alessandra Raffaetà, Rossana Andrade, and Salvatore Orlando. 2016. TPRED: A Spatio-Temporal Location Predictor Framework. In *Proceedings of the 20th International Database Engineering; Applications Symposium (Montreal, QC, Canada) (IDEAS '16)*. ACM, New York, NY, USA, 34–42. <https://doi.org/10.1145/2938503.2938544>
- [13] John Rust. 1988. Maximum likelihood estimation of discrete control processes. *SIAM journal on control and optimization* 26, 5 (1988), 1006–1024.
- [14] R. Trasarti, R. Guidotti, A. Monreale, and F. Giannotti. 2017. MyWay: Location prediction via mobility profiling. *Information Systems* 64 (2017), 350–367. <https://doi.org/10.1016/j.is.2015.11.002>
- [15] Fan Wu, Kun Fu, Yang Wang, Zhibin Xiao, and Xingyu Fu. 2017. A spatial-temporal-semantic neural network algorithm for location prediction on moving objects. *Algorithms* 10, 2 (2017), 37.
- [16] Hao Wu, Ziyang Chen, Weiwei Sun, Baihua Zheng, and Wei Wang. 2017. Modeling Trajectories with Recurrent Neural Networks. In *Proceedings of the Twenty-Sixth International Joint Conference on Artificial Intelligence, IJCAI-17*. 3083–3090. <https://doi.org/10.24963/ijcai.2017/430>
- [17] Di Yao, Chao Zhang, Jianhui Huang, and Jingping Bi. 2017. SerM: A recurrent model for next location prediction in semantic trajectories. In *Proceedings of the 2017 ACM on Conference on Information and Knowledge Management*. 2411–2414.
- [18] Chao Zhang, Keyang Zhang, Quan Yuan, Luming Zhang, Tim Hanratty, and Jiawei Han. 2016. GMove: Group-Level Mobility Modeling Using Geo-Tagged Social Media. In *Proceedings of the 22nd ACM SIGKDD International Conference on Knowledge Discovery and Data Mining (San Francisco, California, USA) (KDD '16)*. Association for Computing Machinery, New York, NY, USA, 1305–1314. <https://doi.org/10.1145/2939672.2939793>
- [19] Wayne Xin Zhao, Ningnan Zhou, Aixin Sun, Ji-Rong Wen, Jialong Han, and Edward Y Chang. 2018. A time-aware trajectory embedding model for next-location recommendation. *Knowledge and Information Systems* 56, 3 (2018), 559–579.
- [20] Brian D. Ziebart, Andrew Maas, J. Andrew Bagnell, and Anind K. Dey. 2008. Maximum Entropy Inverse Reinforcement Learning. In *Proceedings of the 23rd National Conference on Artificial Intelligence - Volume 3 (Chicago, Illinois) (AAAI'08)*. AAAI Press, 1433–1438.

A PROOFS

In the paragraphs below, we present proofs of some claims in the paper.

PROOF. (Proposition 4.1) The probability of a trajectory τ with $\gamma = 1$ is given by

$$\begin{aligned} p(\tau|o, d, \theta) &= \prod_{t=0}^{n-1} p(s_{t+1}|s_t, o, d, \theta) \\ &= \prod_{t=0}^{n-1} \frac{e^{[r(s_t, s_{t+1}) + v_\theta(s_{t+1})]/\alpha}}{\sum_{s' \in \mathcal{A}_{s_t}} e^{[r(s_t, s') + v_\theta(s')]/\alpha}}, \end{aligned}$$

and by observing that

$$e^{v_\theta(s_t)/\alpha} = \sum_{s' \in \mathcal{A}_{s_t}} e^{[r(s_t, s') + v_\theta(s')]/\alpha},$$

we have

$$\begin{aligned} p(\tau|o, d, \theta) &= \prod_{t=0}^{n-1} \frac{e^{[r(s_t, s_{t+1}) + v_\theta(s_{t+1})]/\alpha}}{e^{v_\theta(s_t)/\alpha}} \\ &= e^{\sum_{t=0}^{n-1} [r(s_t, s_{t+1}) + v_\theta(s_{t+1}) - v_\theta(s_t)]/\alpha}. \end{aligned}$$

By further noticing that consecutive terms $v_\theta(s_1) - v_\theta(s_0) + v_\theta(s_2) - v_\theta(s_1) \dots$ cancel out in the sum, and that $v_\theta(s_n) = 0$, we have

$$p(\tau|o, d, \theta) = \frac{e^{\sum_{t=0}^{n-1} r(s_t, s_{t+1})/\alpha}}{e^{v_\theta(s_0)/\alpha}}. \quad \square$$

Proposition A.1 below is an intermediary result which will be used to prove the main Proposition 4.2 in the paper.

PROPOSITION A.1. *If both α and β are scaled by a constant $b \neq 0$, the value function v_θ is also scaled by b .*

PROOF. Let v_θ be a value function defined by

$$v_\theta(s) = \alpha \ln \left(\sum_{s' \in \mathcal{A}_s} e^{[\sum_{k=1}^K \phi(s, s') \beta_k + \gamma v_\theta(s')]/\alpha} \right) \quad \forall s \in \mathcal{S},$$

and let $\alpha' = b\alpha$ and $\beta' = b\beta$. Then

$$\begin{aligned} v'_\theta(s) &= \alpha' \ln \left(\sum_{s' \in \mathcal{A}_s} e^{[\sum_{k=1}^K \phi(s, s') \beta'_k + \gamma v'_\theta(s')]/\alpha'} \right) \\ &= b\alpha \ln \left(\sum_{s' \in \mathcal{A}_s} e^{[\sum_{k=1}^K \phi(s, s') b\beta_k + \gamma v'_\theta(s')]/b\alpha} \right) \\ &= b\alpha \ln \left(\sum_{s' \in \mathcal{A}_s} e^{[\sum_{k=1}^K \phi(s, s') \beta_k + \gamma v'_\theta(s')/b]/\alpha} \right) \end{aligned}$$

$$v'_\theta(s)/b = \alpha \ln \left(\sum_{s' \in \mathcal{A}_s} e^{[\sum_{k=1}^K \phi(s, s') \beta_k + \gamma v'_\theta(s')/b]/\alpha} \right), \quad \forall s \in \mathcal{S},$$

from which we conclude that $v'_\theta(s) = bv_\theta(s)$, $\forall s \in \mathcal{S}$. \square

PROOF. (Proposition 4.2) Let the conditional probability of next locations s' be given by

$$p(s'|s, o, d, \theta) = \frac{e^{[\sum_{k=1}^K \phi(s, s') \beta_k + \gamma v_\theta(s')]/\alpha}}{\sum_{s'' \in \mathcal{A}_s} e^{[\sum_{k=1}^K \phi(s, s'') \beta_k + \gamma v_\theta(s'')]/\alpha}}, \quad \forall s' \in \mathcal{S}.$$

Let $p'(s'|s, o, d, \theta)$ be the conditional probability with $\alpha' = b\alpha$ and $\beta' = b\beta$, in which $b \neq 0$. Then

$$p'(s'|s, o, d, \theta') = \frac{e^{[\sum_{k=1}^K \phi(s, s') \beta'_k + \gamma v'_\theta(s')]/\alpha'}}{\sum_{s'' \in \mathcal{A}_s} e^{[\sum_{k=1}^K \phi(s, s'') \beta'_k + \gamma v'_\theta(s'')]/\alpha'}},$$

and from Proposition 1 we know that $v'_\theta(s) = bv_\theta(s)$, $\forall s \in \mathcal{S}$, so that

$$\begin{aligned} p'(s'|s, o, d, \theta') &= \frac{e^{[\sum_{k=1}^K \phi(s, s') b\beta_k + \gamma bv_\theta(s')]/b\alpha}}{\sum_{s'' \in \mathcal{A}_s} e^{[\sum_{k=1}^K \phi(s, s'') b\beta_k + \gamma bv_\theta(s'')]/b\alpha}} \\ &= \frac{e^{[\sum_{k=1}^K \phi(s, s') \beta_k + \gamma v_\theta(s')]/\alpha}}{\sum_{s'' \in \mathcal{A}_s} e^{[\sum_{k=1}^K \phi(s, s'') \beta_k + \gamma v_\theta(s'')]/\alpha}}, \end{aligned}$$

from which we conclude that $p(s'|s, o, d, \theta) = p'(s'|s, o, d, \theta)$. In this way, since scaling α and β by the same constant $b \neq 0$ does not change the conditional probability of the next location, the likelihood of a trajectory also does not change. Therefore, as scaling of the parameters does not change the likelihood of the data, only the ratios $\beta_1/\alpha, \beta_2/\alpha, \dots$ are identifiable. \square

B GUMBEL PROBABILITY DISTRIBUTION

A continuous random variable $X \in \mathbb{R}$ is said to have a standard Gumbel probability distribution (also known as an extreme value type I distribution) if its cumulative distribution function is given by

$$F(x) = \Pr\{X \leq x\} = e^{-e^{-x}},$$

and density function given by

$$f(x) = \frac{d}{dx} F(x) = e^{-(x+e^{-x})},$$

with expected value $\mathbb{E}[X] = \gamma$ and variance $\mathbb{V}[X] = \pi^2/6$, in which γ here it the Euler-Mascheroni constant (we also use γ for the discount factor in previous sections). If a variable $Y = a + \alpha X$, then Y follows a Gumbel distribution with location a and scale α , with density function

$$f(y) = \frac{1}{\alpha} e^{-\left(\frac{y-a}{\alpha}\right)} e^{-e^{-\left(\frac{y-a}{\alpha}\right)}},$$

with $\mathbb{E}[Y] = a + \alpha\gamma$ and $\mathbb{V}[Y] = \frac{\alpha^2 \pi^2}{6}$. If we assume the location $a = -\alpha\gamma$, then we have a Gumbel variable with $\mathbb{E}[Y] = 0$.

The standard Gumbel variable arises naturally as the maximum of a set of n i.i.d standard exponential variables as $n \rightarrow \infty$. It also is a *max-stable* distribution, i.e., if X_1, X_2, \dots, X_n are i.i.d. Gumbel variables with mean $\mu_1, \mu_2, \dots, \mu_n$ and common scale α , then $Y = \max(X_1, X_2, \dots, X_n)$ is also Gumbel with scale α and expected value given by

$$\mathbb{E}[Y] = \alpha \ln \sum_{i=1}^n e^{\mu_i/\alpha}.$$

It can also be shown that the probability that variable X_i assumes the maximum value is given by

$$\Pr\{X_i \geq X_j, j = 1, \dots, n, j \neq i\} = \frac{e^{\mu_i/\alpha}}{\sum_{i=j}^n e^{\mu_j/\alpha}}.$$